Journal of Materials Chemistry A

Accepted Manuscript

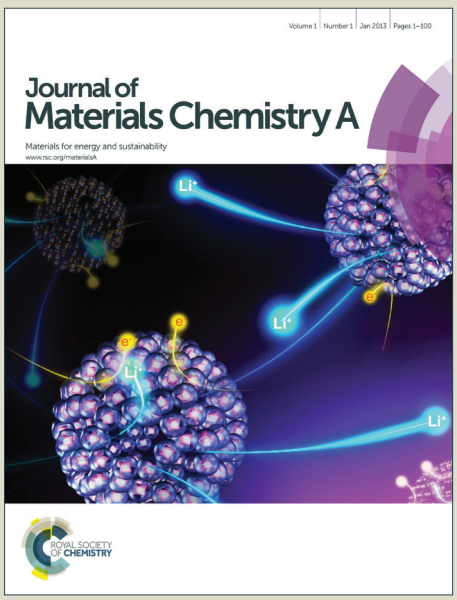

ROYAL SOCIETY OF CHEMISTRY

www.rsc.org/materialsA

Journal Name

RSCPublishing

ARTICLE

Supercapacitive Energy Storage Performance of Molybdenum Disulfide Nanosheets Wrapped with Microporous Carbons

Cite this: DOI: 10.1039/x0xx00000x

Received 00th January 2012,
Accepted 00th January 2012

DOI: 10.1039/x0xx00000x

www.rsc.org/

Qunhong Weng,[a,b]* Xi Wang,[a] Xuebin Wang,[a] Chao Zhang,[a] Xiangfen Jiang,[a] Yoshio Bando [a] and Dmitri Golberg [a,b]*

We conceived a material composed of a pseudocapacitive core and an electrostatic double-layer capacitive porous shell for advanced electrochemical energy storage. As a proof-of-concept, the MoS_2 nanosheets wrapped with microporous carbons (MoS_2@MPC) were fabricated via a three-step strategy and applied in supercapacitor research. The structures exhibit high specific capacitance, rate capability and cycling stability due to the combined involvements of both structural portions under the electrochemical charge storage and release procedures.

Introduction

Molybdenum disulfide (MoS_2) is one of the "hottest" semiconducting transition metal dichalcogenides with an indirect band gap of 1.2 eV. It is stacked by three-atom S-Mo-S layers through van der Waals interactions.[1] Due to this structural feature, it acts like graphite and hexagonal boron nitride that can be used as a solid lubricant or exfoliated to form mono- or few-layered nanosheets.[2] Compared with bulk MoS_2, the two-dimensional (2D) MoS_2 nanosheets exhibit wider band gaps and unique optical properties, such as photoluminescence. Being thinned down to monolayer, the material becomes a direct band gap semiconductor.[3,4]

Among the application fields that MoS_2 materials have emerged, such like electronics, catalysis and energy storages,[5] recent studies have shown that these materials hold a promise for efficient Li/Na ions storage and release while they are hybridized with graphene.[5–8] With respect to the other important electrochemical energy storage modes, the concept of using MoS_2 as a supercapacitor material is in its infancy. Faradaic charge transfer has already been observed in several MoS_2-based material systems.[9,10] Since the specific capacitance of MoS_2 alone is limited,[9,11] efforts to increase its capacitance have generally relied on its hybridization with other materials, like graphene,[10] multi-walled carbon nanotubes (MWCNTs),[12] and conducting polymers.[13,14] And indeed, the apparent capacitances were enhanced enormously. However, the roles and contributions of MoS_2 in such hybrid systems are still unclear. Further improvement of the rate capability and cycling life are also desired for the development of a practical MoS_2-based supercapacitor.

Herein, we design and fabricate a novel core-shell structure for high-performance supercapacitive energy storage. This structure is made of a pseudocapacitive 2D material (MoS_2 nanosheets) as the core, and metal-organic framework (MOF)-derived microporous carbons as the shell (MoS_2@MPC). Thus, the hybrid takes an advantage of employing both the electrostatic double-layer electrolyte ion storage on stable carbon surfaces and the high-capacitance and pseudocapacitive properties of MoS_2. Our results show that the designed MoS_2@MPC structure exhibits a high specific capacitance of 189 F g^{-1} at a current density of 1 A g^{-1}, compared to only 43 F g^{-1} for the mechanically mixed MoS_2-MPC material with the same composition. It is perfectly rate-scalable, and can maintain 98 % of the specific capacitance after 3000 charge-discharge cycles, highlighting the effectiveness of the present structural design which allows avoiding quick capacitance degeneration that the conventional pseudocapacitive materials are usually facing. The obvious reversible redox peaks seen in their cyclic voltammetry (CV) curves imply the involvement of the pseudocapacitive MoS_2 cores during the energy storage cycles.

Experimental details

Fabrication of MoS_2 nanosheets. MoS_2 nanosheets were fabricated using mechanical exfoliation of bulk MoS_2 in N-methylpyrrolidinone (NMP) similar to the method described in Ref. 2. Briefly, ~ 0.6 g MoS_2 powders were added in 100 mL NMP. The mixture was sonicated with a tip sonicator for 3 h. Then, the suspension was centrifuged at 2000 rpm for 20 min and ~3/4 supernatants were collected. The obtained MoS_2 suspension was further centrifuged at 12500 rpm to remove the solvent and washed by ethanol 3 times. After vacuum drying at 80 ^oC overnight, ~15 mg of the MoS_2 nanosheet powder was obtained. This process was repeated to collect ~30 mg sample during the following steps.

Preparation of MoS_2@ZIF-8. The obtained MoS_2 nanosheets were re-dispersed in ethanol to form MoS_2/ethanol suspensions under sonication. A variety of mass ratios for the reactants and solvent systems were tried to wrap MoS_2 nanosheets with ZIF-8 (chemical formula: $Zn(MeIM)_2$; $MeIM^-$ = 2-Methylimidazole) layers.[15] The optimized fabrication condition was found as follows: 100 mL 0.3 g L^{-1} MoS_2/ethanol suspension was added to 400 mL 0.83 g L^{-1} $Zn(Ac)_2 \cdot 2H_2O$/ethanol solution under stirring. Then, 100 mL 10.0 g L^{-1} MeIM/water solution was added to initiate the reaction. After 1 h, the product (65 mg) was collected after centrifugation (5000 rpm), washed by ethanol 3 times and dried at 80 ^oC overnight. Other mass ratios, e.g. 0.18:10:30 and 0.36:10:30 for

MoS_2, $Zn(Ac)_2{\cdot}2H_2O$ and MeIM always led to the formation of MoS_2@ZIF-8 and ZIF-8 nanocrystal mixtures. Using sole water as the reaction solvent was found to be ineffective to coat ZIF-8 layers on MoS_2 surfaces.

Preparation of MoS_2@MPC. To convert the ZIF-8 coatings into microporous carbons (MPC), the synthesized 65 mg MoS_2@ZIF-8 samples were calcined at 900 °C for 2 h under the protection of Ar flow. The heating rate was set as 3.3 °C min^{-1}. Finally, the system was cooled to room temperature naturally and the MoS_2@MPC product (~38 mg) was collected.

Material characterizations. The morphologies and chemical compositions of the materials were analyzed using SEM (JSM-6700F), HRTEM (JEM-3000F, 300 kV), EDS (JEOL), XPS (PHI Quantera SXM), XRD (Rigaku Ultima III diffractometer, Cu Kα) and Raman (Horiba Jobin–Yvon T6400, excited by a 514.5 nm laser) spectroscopies.

Electrochemical measurements. Electrochemical measurements were conducted on a Solartron potentiostat with a standard three-electrode electrochemical cell. Platinum wire electrode and Ag/AgCl (saturated KCl) electrode were used as the counter and reference electrodes, respectively. The electrolyte was a 1 M H_2SO_4 aqueous solution. The working electrode was prepared by casting a sample onto a glassy carbon electrode (i.d. = 3 mm). Typically, 2 mg of a sample was firstly added to 0.8 mL ethanol/DI water (3:1) with 20 µL 5 % Nafion solution. The mixture was sonicated for 10 min to form a uniform suspension, from which 4 µL was dropped on the glassy carbon electrode. After drying, the Nafion binder was further fixed under the treatment at 60 °C for 10 min. Before all electrochemical experiments, the working electrodes were activated by cyclic voltammetry method with a scanning rate of 100 mV s^{-1} for 500 circles. CV (5, 20, 50 and 100 mV s^{-1}) and galvanostatic charge/discharge (1–20 A g^{-1}) tests were performed to evaluate the electrochemical and supercapacitor behaviors. All potential values for electrochemical measurements are reported relative to the Ag/AgCl (saturated KCl) reference electrode with a potential window of 0–0.8 V. Cyclic stabilities were characterized using galvanostatic charge/discharge measurements over 3000 cycles at a charge/discharge rate of 10 A g^{-1}.

The gravimetric specific capacitance C_g was calculated based on the following equation:

$C_g = I \times \Delta t / (m \times \Delta V)$

Where I, Δt, ΔV and m denote the applied current, discharge time, voltage change and the mass of the active material, respectively.

Results and discussion

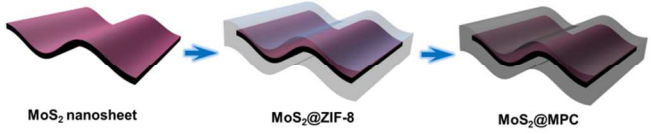

Fig. 1 Schematic illustration of MoS_2@MPC preparation. Mechanically exfoliated MoS_2 nanosheets were firstly coated with ZIF-8, a metal-organic framework. Then, the ZIF-8 coatings were converted to microporous carbons (MPC) by direct carbonization.

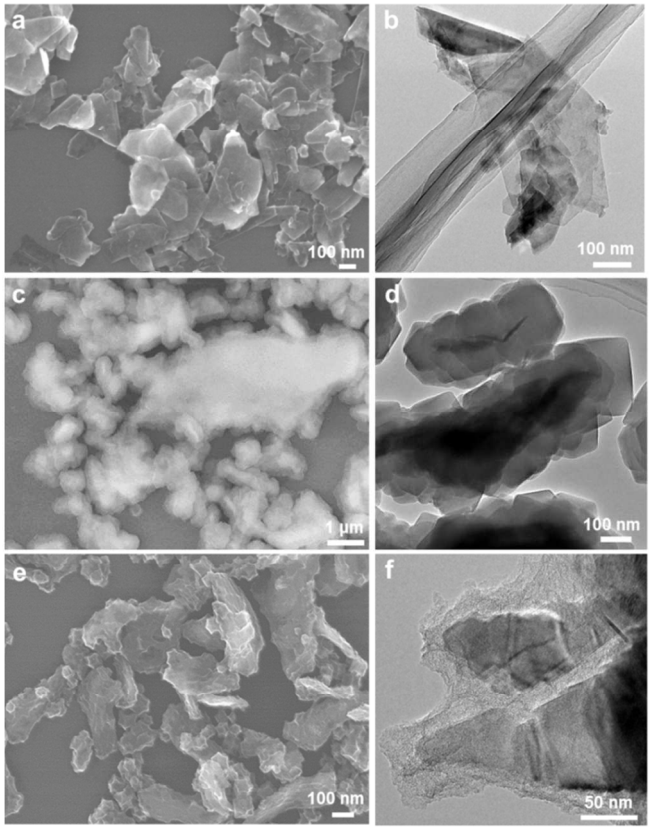

Fig. 2 SEM images of MoS_2 nanosheets (a), MoS_2@ZIF-8 (c) and MoS_2@MPC (e); TEM images of MoS_2 nanosheets (b), MoS_2@ZIF-8 (d) and MoS_2@MPC (f).

The MoS_2@MPC materials were prepared via a three-step procedure (Fig. 1). Firstly, the few-layered MoS_2 were produced under sonication-induced exfoliation of bulk MoS_2 powders in N-methylpyrrolidinone (NMP).[2] Both SEM and TEM analyses (Fig. 2a,b) show the typical sheet-like structures of the exfoliated MoS_2. The observed lateral sizes of the sheets were usually in the range of 0.1 to 5 µm, while extra-large sheets up to ~10 µm were also occasionally found. The HRTEM and SAED images of the obtained MoS_2 nanosheets (Fig. 3a,c) confirm the typical hexagonal lattice with the (100) distance of 0.27 nm. To form highly-crystalline ZIF-8 coatings on the MoS_2 nanosheet surfaces, a mixed-solvent-based reaction at room temperature was performed with the optimized MoS_2:$Zn(Ac)_2{\cdot}2H_2O$: MeIM mass ratio of 0.9:10:30. Decreasing the proportion of MoS_2 led to a large amount of ZIF-8 nanocrystals, see Fig. S1, ESI. Furthermore, a ratio of 1:4 (v/v) for H_2O:ethanol was found to be a suitable solvent for the present coating reaction. No MoS_2@ZIF-8 products could be formed if only H_2O was adopted as a solvent instead of the H_2O-ethanol system (Fig. S1, ESI), which is different from the growth process reported elsewhere.[16] The sharp corners of the MOF coatings peculiar to ZIF-8 single crystal characteristics indicate the high crystallinity of the formed ZIF-8 coatings with a thickness of ~100 nm, as shown in Fig 2c,d. Final MoS_2@MPC materials were obtained by a direct carbonization treatment at 900 °C under the protection of Ar flow (Fig. 2e,f). At this temperature, the MeIM ligands in ZIF-8 were converted to microporous carbons,[17] while Zn(II) was reduced to Zn(0) and further removed by evaporation.

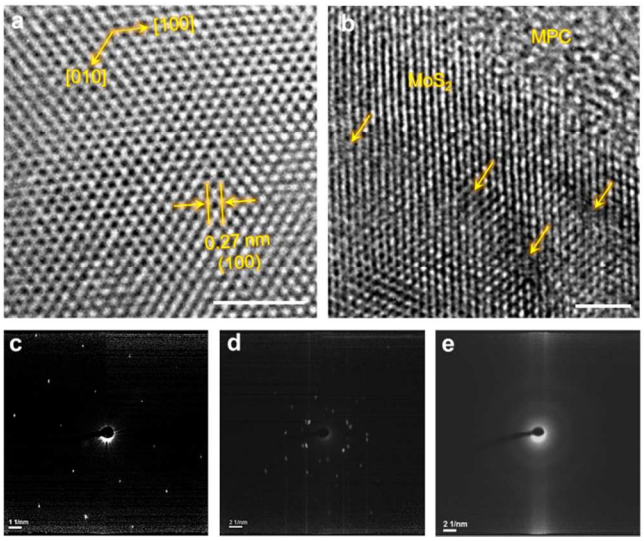

Fig. 3 High-magnification HRTEM images of MoS_2 nanosheets (a) and MoS_2@MPC (b). The arrows marked in (b) show the lattice defects in MoS_2. The scale bars are 2 nm. Typical SAED patterns of MoS_2 nanosheets (c), MoS_2 cores in MoS_2@MPC (d) and MPC shells in MoS_2@MPC (e).

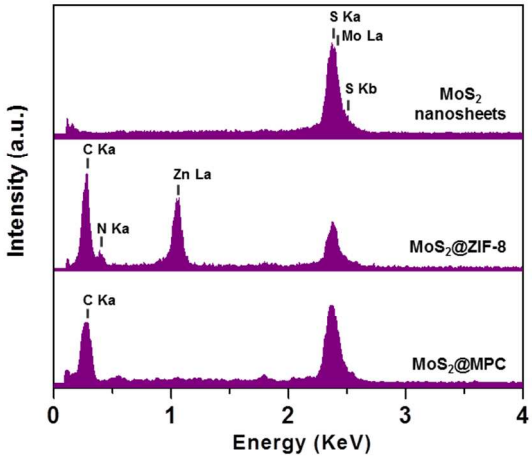

Fig. 4 EDS spectra of MoS_2 nanosheets, MoS_2@ZIF-8, and MoS_2@MPC.

The EDS spectra further confirm that the obtained MoS_2@MPC products are mainly composed C, Mo and S with a mole ratio close to 75:9:17; i.e., the carbon component takes ~40 wt % of the total MoS_2@MPC mass. Other components, like N and Zn, which are present in MoS_2@ZIF-8, were eliminated after the calcination treatment (Fig. 4) except a trace amount of O. It was reported that such treatment of MoS_2 nanosheets would introduce defects into their surfaces.[18] Our HRTEM observations also confirm this point. Although the structures of MoS_2 cores were generally kept stable after 900 ^oC calcination in Ar atmosphere, as also documented by the XRD and Raman spectra shown in Fig. 5c and S3 (ESI), respectively, there were indeed considerable structural defects seen in the hexagonal lattice along the [002] zone axis of MoS_2 nanosheets (Fig. 3b). In Fig. 3d, the SAED pattern of the MoS_2 cores show a partial polycrystalline feature, also confirming the increased defect density within the MoS_2 phase of the prepared MoS_2@MPC. This change is likely caused by the reactions between the surface MoS_2 layers and gaseous molecules decomposed or trapped by ZIF-8 at high temperatures. The MPC shell structures, as revealed by HRTEM (Fig. 3b), SAED (Fig. 3e) and XRD images (Fig. 5c), are amorphous.

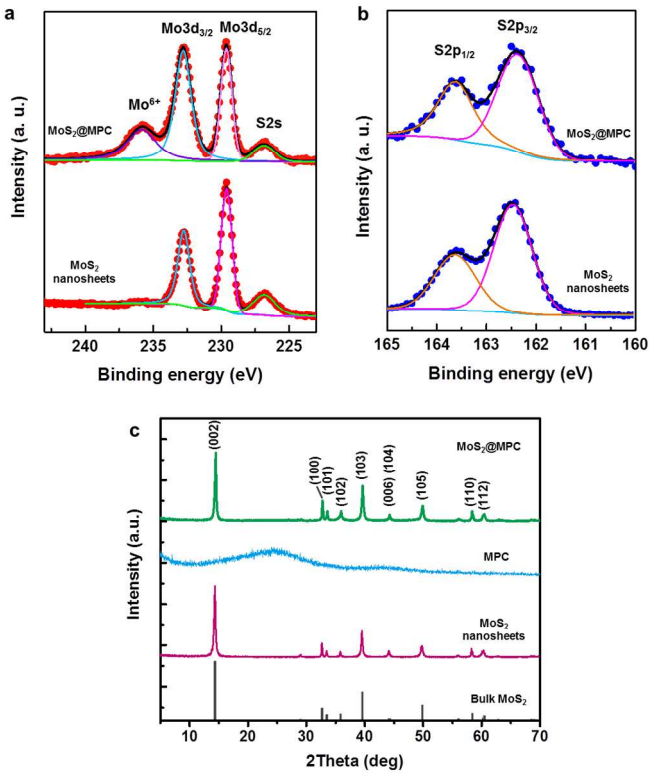

Fig. 5 Mo3d, S2s (a) and S2p (b) XPS spectra of MoS_2@MPC and MoS_2 nanosheets. (c) XRD patterns (from top to bottom) of MoS_2@MPC, MPC, MoS_2 nanosheets and standard bulk MoS_2 (JCPDS 651951) diffraction pattern.

XPS analysis was performed to understand the chemical environment of the MoS_2 components in MoS_2@MPC product. Fig. 5a shows the Mo3d XPS spectrum of the MoS_2@MPC sample. There are two Mo oxidation states in the spectrum; the ones at 229.6 and 232.8 eV are the $Mo3d_{5/2}$ and $Mo3d_{3/2}$ of Mo(IV) component arisen from Mo-S structures, while the peak at 236 eV only shown in the MoS_2@MPC is caused by the $Mo3d_{3/2}$ of Mo(VI) components (the structures related with the defects in MoS_2, e.g. Mo–O phase).[19] These defects were introduced during the final conversion process of MOF coatings to MPC at a high temperature. S2p XPS spectra (Fig. 5b) reveal typical S2p3/2 and S2p1/2 peaks of the MoS_2 phase.

The as-prepared MoS_2@MPC core-shell compounds were used as the active materials in a working electrode for electrochemical and supercapacitance measurements in an aqueous electrolyte (1 M H_2SO_4 solution). Fig. 6a shows the CVs obtained for the MoS_2@MPC materials at various scanning rates within a potential range of 0–0.8 V. Generally, the current density tends to increase with the increase of the scanning rate. The CV curves retain its shape even at high scan rates, indicating a good high-rate performance of the active materials. As can be further discovered from these characteristic CV curves, the materials display near-rectangular curve shapes and the presence of reversible peaks, which are arisen from the MoS_2 pseudocapacitive behaviors. It was reported that the Mo atoms at the MoS_2 edges may change their valence states during the electrochemical redox processes,[10] thus providing important contributions to the total capacitance. For a comparison, we also investigated the CV behaviors of the mechanically mixed MoS_2

nanosheets and MPC at a mass ratio of 3:2 (Fig. 6b). The resultant near-rectangular shapes of the CV curves indicate a dominating and ideal electrostatic double-layer capacitive characteristic. No redox peaks are displayed by this MoS_2+MPC sample, evidencing no pseudocapacitive contribution for the large-sized, few-layered and highly-crystalline MoS_2 nanosheets.

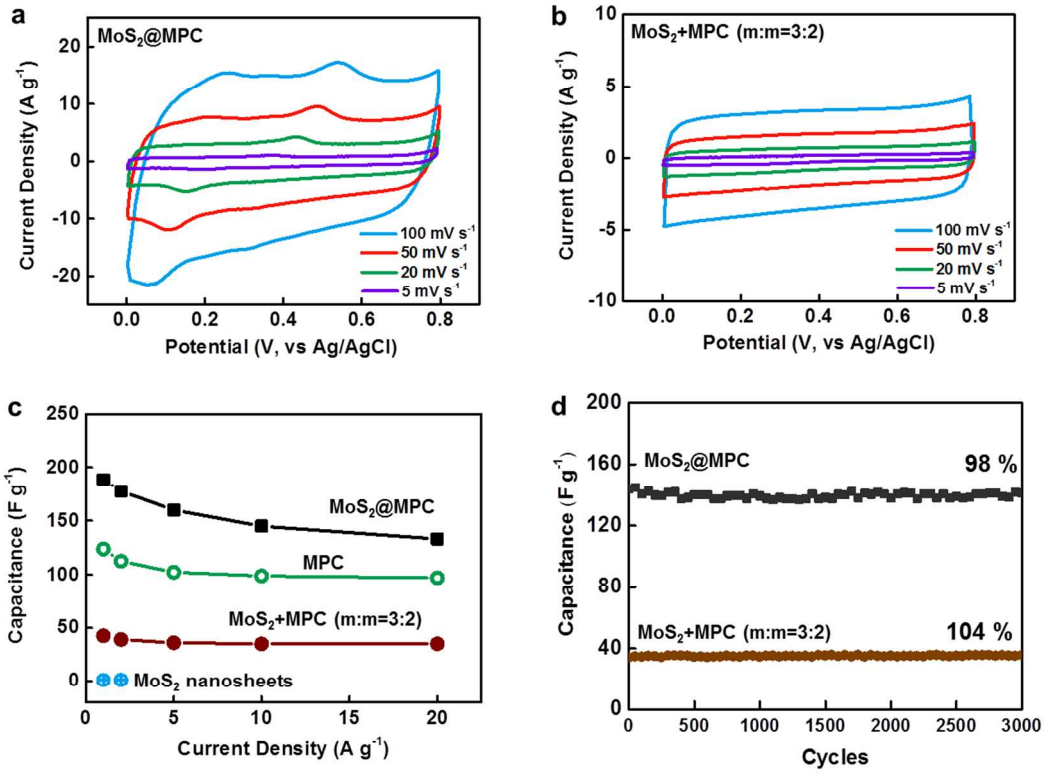

Fig. 6 CVs of MoS_2@MPC (a) and a mixture of MoS_2 and MPC (m:m = 3:2) (b) at different scan rates. (c) Specific capacitance of the MoS_2@MPC sample, MPC, the mixture of MoS_2 and MPC (m:m = 3:2) and MoS_2 nanosheets (treated at 900 °C in Ar) at various current densities. (d) Cycling stability of MoS_2@MPC and the mixture of MoS_2 and MPC (m:m = 3:2). The current density in (d) is 10 A g^{-1}.

The gravimetric specific capacitance of the materials was measured and calculated using the discharge portion of the galvanostatic charge−discharge profiles. Such profiles and calculated specific capacitance values at different current densities are illustrated in Fig. 6c and S6 (ESI), respectively. At 1 A g^{-1}, MoS_2@MPC delivers a very high specific capacitance of 189 F g^{-1}, which is 4.4-fold larger than that of the MoS_2+MPC sample, and also much higher than the MPC at any given current densities. It is noted that the exfoliated MoS_2 nanosheets, also treated under 900 °C for 2 h in Ar, show negligible specific capacitance (<1 F g^{-1}) at the same testing conditions. With the increase of discharge current from 1 to 20 A g^{-1}, it can still preserve a specific capacitance as high as 133 F g^{-1}, which is ~70.5 % retention and comparable to the ideal electrostatic double-layer capacitive MPC layers (78.4 %). The core-shell MoS_2@MPC structure exhibits an excellent cyclic stability; less than 2 % specific capacitance loss was observed for the materials after 3000 charge–discharge cycles (Fig. 6d). It is noted that a small increase in the specific capacitance (4 %) occurred for the mechanically mixed MoS_2+MPC sample, possibly due to the effect of a long activation process. Such impressive rate and cycling properties of MoS_2@MPC are among the best performances for the reported MoS_2-C (see Table S1, ESI) and MoS_2-polymer hybridized materials,[13,14] also very close to those of the pure carbon-based supercapacitors that we have developed recently.[20]

As one may see, the reported MoS_2-C composites were prepared *via* growing MoS_2 on graphene and MWCNT surfaces, while MoS_2-polymer were obtained by growing the conducting polymers, like polyaniline and polypyrrole, on MoS_2 surfaces. Such material design can certainly maximize the pseudocpacacitive activities of MoS_2 or the polymer component, but is not helpful to overcome the main challenge that pseudocpacacitive materials are always facing (faster loss of specific capacitance during cycling). For instance, MoS_2-rGO with the MoS_2 hydrothermally grown on GO surfaces, as a typical composite of such structure design, shows a high initial specific capacitance of 265 F g^{-1} at 10 mV s^{-1} in 1.0 M $HClO_4$, while it only retains 70 % specific capacitance after 1000 cycles.[10] The important role of MPC shells in the present hybrid structure during charge storage is supposed to their effects on pseudocpacacitive core structure protections, ions enrichment in the electrolyte and providing a dense electron transport network. Similar enhancement was also observed in MOF-encapsulated Pd nanocrystals for higher H_2 uptakes than Pd cores and MOF coatings separately.[21] Therefore, owing to the combined characteristics of effective pseudocpacacitive MoS_2 cores and highly porous MPC coatings, MoS_2@MPC exhibits not only high capacitance but also high-rate performance and long cycling stability. These are the key factors for their promising applications in high-demand electrochemical energy storages.

Conclusions

In summary, a structure composed of a pseudocapacitive core (MoS_2 nanosheets) and an electrostatic double-layer capacitive shell (MOF-derived microporous carbons) was designed and fabricated via a three-step route toward the achievement of effective and long-life supercapacitive energy storage. The atomic structures and chemical compositions of the materials were analyzed by SEM, TEM, EDS, XPS and Raman spectroscopies. The cyclic voltammetry tests confirm the synergistic effects of both core and porous shell portions during the electrochemical energy storage

processes. Taken the advantages of the created structure, a relatively high capacitance of 189 F g^{-1} was achieved, which is a 4.4-fold enhancement compared to such figure for a simple mechanical mixture of MoS_2 nanosheets and microporous carbons. Combining with the material's high-rate and long cyclic performances, the proposed design allows one to avoid quick specific capacitance degeneration for a pseudocapacitive material, and holds a high promise for future electrochemical energy storage applications.

Notes and references

[a] World Premier International Center for Materials Nanoarchitectonics (WPI-MANA), National Institute for Materials Science (NIMS), Namiki 1-1, Tsukuba, Ibaraki 305-0044, Japan. weng.qunhong@nims.go.jp; golberg.dmitri@nims.go.jp

[b] Graduate School of Pure and Applied Sciences, University of Tsukuba, Tennodai 1, Tsukuba, Ibaraki 305-0005, Japan.

Electronic Supplementary Information (ESI) available: Detailed SEM characterizations, Raman spectra, additional XRD data, galvanostatic charge-discharge curves and Summary of the related supercapacitor performances in Refs. See DOI: 10.1039/c000000x/

1 R. Tenne, L. Margulis, M. Genut, G. Hodes, *Nature*, 1992, **360**, 444.
2 J. N. Coleman, M. Lotya, A. O'Neill, S. D. Bergin, P. J. King, U. Khan, K. Young, A. Gaucher, S. De, R. J. Smith, I. V. Shvets, S. K. Arora, G. Stanton, H. Y. Kim, K. Lee, G. T. Kim, G. S. Duesberg, T. Hallam, J. J. Boland, J. J. Wang, J. F. Donegan, J. C. Grunlan, G. Moriarty, A. Shmeliov, R. J. Nicholls, J. M. Perkins, E. M. Grieveson, K. Theuwissen, D. W. McComb, P. D. Nellist and V. Nicolosi, *Science*, 2011, **331**, 568.
3 T. Li and G. Galli, G. *J. Phys. Chem. C*, 2007, **111**, 16192.
4 A. Splendiani, L. Sun, Y. Zhang, T. Li, J. Kim, J. Chim and F. Wang, *Nano Lett.*, 2010, **10**, 1271.
5 M. Chhowalla, H. S. Shin, G. Eda, L. J. Li, K. P. Loh and H. Zhang, *Nat. Chem.*, 2013, **5**, 263.
6 H. Hwang, H. Kim, and J. Cho, *Nano Lett.*, 2011, **11**, 4826.
7 K. Chang and W. Chen, *ACS Nano*, 2011, **5**, 4720.
8 D. Lamuel, B. Romil and S. Gurpreet, *ACS Nano*, 2014, **8**, 1759.
9 J. M. Soon and K.P. Loh, Electrochem. *Solid-State Lett.*, 2007, **10**, A250.
10 E. G. da Silveira Firmiano, A. C. Rabelo, C. J. Dalmaschio, A. N. Pinheiro, E. C. Pereira, W. H. Schreiner, E. R. Leite, *Adv. Energy Mater.*, 2014, **4**, 1301380.
11 K. Krishnamoorthy, G. K. Veerasubramani, S. Radhakrishnan and S. J. Kim, *Mater. Res. Bull.*, 2014, **50**, 499.
12 K. J. Huang, L. Wang, J. Z. Zhang, L. L. Wang and Y. P. Mo, *Energy*, 2014, **67**, 234.
13 K. J. Huang, L. Wang, Y. J. Liu, H. B. Wang, Y. M. Liu and L. L. Wang, *Electrochim. Acta*, 2013, **109**, 587.
14 G. Ma, H. Peng, J. Mu, H. Huang, X. Zhou and Z. Lei, *J. Power Sources*, 2013, **229**, 72.
15 K. S. Park, Z. Ni, A. P. Côté, J. Y. Choi, R. Huang, F. J. Uribe-Romo, H. K. Chae, M. O'Keeffe and O. M. Yaghi, *Proc. Natl. Acad. Sci. U. S. A.*, 2006, **103**, 10186.
16 X. Huang, B. Zheng, Z. Liu., C. Tan., J. Li, B. Chen, H. Li, J. Chen, X. Zhang, Z. Fan, W. Zhang, Z. Guo, F. Huo, Y. Yang, L. Xie, W. Huang, and H. Zhang, *ACS Nano*, 2014, **8**, 8695.
17 W. Chaikittisilp, M. Hu, H. Wang, H.-S. Huang, T. Fujita, K. C.-W. Wu, L.-C. Chen, Y. Yamauchi and K. Ariga, *Chem. Commun.*, 2012, **48**, 7259.
18 H. Nan, Z. Wang, W. Wang, Z. Liang, Y. Lu, Q. Chen, D. He, P. Tan, F. Miao, X. Wang, X. Wang and Z. Ni, *ACS Nano*, 2014, **8**, 5738.
19 X. Yang, W. F. Fu, W. Q. Liu, J. H. Hong, Y. Cai, C. H. Jin, M. S. Xu, H. B. Wang, D. R. Yang and H. Z. Chen, *J. Mater. Chem. A*, 2014, **2**, 7727.
20 X. Wang, Y. Zhang, C. Zhi, X. Wang, D. Tang, Y. Xu, Q. Weng, X. Jiang, M. Mitome, D. Golberg and Y. Bando, *Nat. Commun.*, 2013, **4**, 2905.
21 G. Li, H. Kobayashi, J. M. Taylor, R. Ikeda, Y. Kubota, K. Kato, M. Takata, T. Yamamoto, S. Toh, S. Matsumura and H. Kitagawa, *Nat. Mater.*, 2014, **13**, 802.

Table of Contents

Supercapacitive Energy Storage Performance of Molybdenum Disulfide Nanosheets Wrapped with Microporous Carbons

Qunhong Weng,[a,b]* Xi Wang,[a] Xuebin Wang,[a] Chao Zhang,[a] Xiangfen Jiang,[a] Yoshio Bando [a] and Dmitri Golberg [a,b]*

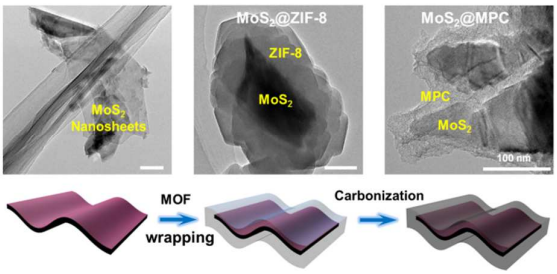

A structure composed of a pseudocapacitive core (MoS_2 nanosheets) and an electrostatic double-layer capacitive porous shell (MOF-derived microporous carbons) was developed for advanced electrochemical energy storage.